AGU PUBLICATIONS

Geophysical Research Letters

RESEARCH LETTER
10.1002/2017GL075707

Key Points:
- Meltwater flows through, and therefore discharges from, the firn aquifer upslope from Helheim Glacier
- Borehole dilution tests reveal the meltwater flow zone within and quantify discharge through the ice sheet firn
- Firn pore space is a short-term (<30 years) storage reservoir in areas where firn aquifers exist

Supporting Information:
- Supporting Information S1

Correspondence to:
O. Miller,
olivia.miller@utah.edu

Citation:
Miller, O., Solomon, D. K., Miège, C., Koenig, L., Forster, R., Schmerr, N., … Montgomery, L. (2018). Direct evidence of meltwater flow within a firn aquifer in southeast Greenland. *Geophysical Research Letters*, *45*, 207–215. https://doi.org/10.1002/2017GL075707

Received 26 SEP 2017
Accepted 1 DEC 2017
Accepted article online 8 DEC 2017
Published online 11 JAN 2018

Direct Evidence of Meltwater Flow Within a Firn Aquifer in Southeast Greenland

Olivia Miller[1], D. Kip Solomon[1], Clément Miège[2], Lora Koenig[3], Richard Forster[2], Nicholas Schmerr[4], Stefan R. M. Ligtenberg[5], and Lynn Montgomery[6]

[1]Department of Geology and Geophysics, University of Utah, Salt Lake City, UT, USA, [2]Geography Department, University of Utah, Salt Lake City, UT, USA, [3]National Snow and Ice Data Center, University of Colorado Boulder, Boulder, CO, USA, [4]Department of Geology, University of Maryland, College Park, MD, USA, [5]Institute for Marine and Atmospheric research Utrecht, Utrecht University, Utrecht, Netherlands, [6]Atmospheric and Oceanic Science Department, University of Colorado Boulder, Boulder, CO, USA

Abstract Within the lower percolation zone of the southeastern Greenland ice sheet, meltwater has accumulated within the firn pore space, forming extensive firn aquifers. Previously, it was unclear if these aquifers stored or facilitated meltwater runoff. Following mixing of a saline solution into boreholes within the aquifer, we observe that specific conductance measurements decreased over time as flowing freshwater diluted the saline mixture in the borehole. These tests indicate that water flows through the aquifer with an average specific discharge of 4.3×10^{-6} m/s ($\sigma = 2.5 \times 10^{-6}$ m/s). The specific discharge decreases dramatically to 0 m/s, defining the bottom of the aquifer between 30 to 50 m depth. The observed flow indicates that the firn pore space is a short-term (<30 years) storage mechanism in this region. Meltwater flows out of the aquifer, likely into nearby crevasses, and possibly down to the base of the ice sheet and into the ocean.

Plain Language Summary Across some parts of the Greenland ice sheet, meltwater generated at the snow surface travels downward through a layer of compacting snow and firn (older snow). From the bottom of the firn layer (about 30 m), the meltwater fills up available pore space and creates a firn aquifer. We drilled through this aquifer in several places to determine if and how much water was flowing. We confirmed that meltwater is flowing through the firn aquifer, inferring that this water is also leaving the aquifer at its downstream edge. Our method also confirms the bottom of the aquifer as we found no flow happening below it. Water leaving the aquifer likely flows into crevasses downhill and is routed toward the edge of the ice sheet. Our measurements can be used to model if water-filled crevasses could break open and allow water to flow inside the ice sheet, perhaps toward its base and later out into the ocean.

1. Introduction

The Greenland ice sheet is losing mass due to surface meltwater runoff and ice discharge, with important implications for sea level rise (Shepherd et al., 2012). The surface of the Greenland ice sheet (GrIS) has experienced warming of ~0.5°C/decade (Hall et al., 2013), accelerating mass loss (Vaughan et al., 2013). Mass loss results from surface meltwater runoff and ice discharge to the ocean, with surface mass balance processes becoming increasingly dominant (Enderlin et al., 2014; van den Broeke et al., 2009). Surface melt area extent has increased since the late 1950s (Fettweis et al., 2011). While meltwater from the GrIS contributes to sea level rise, how and when surface meltwater reaches the ocean is poorly constrained, particularly within the expanding percolation zone (Koenig et al., 2015; Rennermalm et al., 2013; Tedesco, 2013).

Longer term (multiannual) meltwater storage occurs when infiltrated meltwater freezes at depth within cold firn, thereby buffering sea level rise (Harper et al., 2012; Parry et al., 2007; Pfeffer, 1991). Although modeling studies show that 45% of meltwater refreezes in firn (Ettema et al., 2009), firn capacity varies spatially and temporally (de la Peña et al., 2015; Lindbäck et al., 2015; Machguth et al., 2016; van Angelen et al., 2013). Meltwater discharge occurs when meltwater flows through the glacial hydrologic system and contributes to sea level rise (Chu, 2014; Lewis & Smith, 2009; Smith et al., 2015). This process can occur over shorter (daily-seasonal) or longer time scales (annually, as described in this manuscript).

Across the southeast GrIS percolation zone, snowmelt infiltrates into the upper layers of the ice sheet and fills available pore space above the firn-ice transition, forming large unconfined aquifers that persists throughout

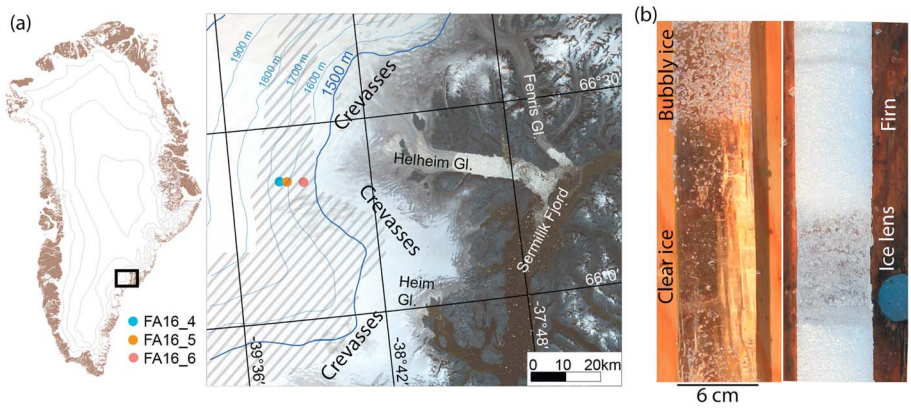

Figure 1. (a) Site map showing sites where we collected firn cores and conducted borehole dilution tests (FA16_4, FA16_5, and FA16_6) in 2016. Grey lines indicate aquifer extent. Elevation contours from Helm et al. (2014) and Landsat-8 image from 3 August 2016 (U.S. Geological Survey). (b) Photos of the different firn/ice core types illustrating bubbly ice, clear ice, firn, and ice lenses lying on top of wooden boards. Stratification of ice types is shown in Figure 3.

the year (Forster et al., 2014; Koenig et al., 2014). Firn aquifers form where melt rates are high, and high accumulation provides pore space and insulation for the water to persist through cold winters (Kuipers Munneke et al., 2014; Miège et al., 2013). The aquifer covers between 22,000–90,000 km^2 (~4% of ice sheet area) and, if released into the ocean, would contribute about 0.4 mm of sea level rise globally (Forster et al., 2014; Koenig et al., 2014; Miège et al., 2016; Steger et al., 2017).

The effect the firn aquifer has on meltwater runoff has been unclear. Two end-member pathways for the stored meltwater to exit the aquifer are (1) the aquifer drains constantly into the englacial and/or subglacial hydrologic networks including crevasses and moulins that may reach the ice sheet bed or (2) the aquifer stores water in pore space until all available pore space is filled and/or a threshold is met (Koenig et al., 2014; Poinar et al., 2017). Total firn meltwater storage capacity across the percolation zone of the GrIS is estimated between ~300 and 1,200 Gt from field observations of firn structure and meltwater retention (Harper et al., 2012).

Field observations of highly permeable firn (~10^{-12} to 10^{-10} m^2) and a sloping (less than ~2°) water table (Forster et al., 2014; Koenig et al., 2014; Miller et al., 2017) suggest that meltwater should flow within the aquifer if a connected network of pores is maintained. According to Darcy's law, the hydraulic conductivity and the hydraulic gradient within an aquifer control the specific discharge. Meltwater flow through the aquifer can be accompanied by discharge and/or a change in storage. Crevasses lie directly downstream from an aquifer in southeast Greenland and may allow meltwater to reach the ice sheet bed (Poinar et al., 2017). Thus, characterizing water flow within the aquifer is critical to determining whether the aquifer stores or transmits meltwater into other englacial or subglacial hydrologic networks.

Here we present the first direct evidence that fluid flow occurs within the aquifer accompanied by estimates of specific discharge and average linear velocity. We also identify the depth of the bottom of the aquifer (firn/ice transition) where fluid flow ceases in glacier ice (pores close off). These measurements support a direct connection between meltwater within the firn aquifer and an englacial or subglacial drainage system. This connection may have substantial implications on ice dynamics in this region if discharging meltwater reaches the base of the ice sheet through crevasses, where it can lead to increased ice velocity.

2. Methods

We collected firn cores at three sites along a glacier flow line ~50 km upslope from the terminus of Helheim Glacier, southeastern Greenland in July and August 2016 (Figure 1; see supporting information for a more detailed explanation of methods). At this site, the ice is approximately 1 km thick, and snow accumulation rates simulated by regional climate models range from 1 to 4 m water equivalent per year (Burgess et al., 2010; Ettema et al., 2009; van Angelen et al., 2012). Cores were collected using a lightweight thermal drill developed by Jay Kyne and logged for density and stratigraphy. We observed four main firn/ice types

between the surface and 50 m depth: firn, ice lenses, bubbly ice, and clear ice (Figure 1). Firn is snow that lasts longer than an ablation season without transforming to ice (Cogley et al., 2011). Ice lenses form as surface meltwater infiltrates and refreezes in snow and firn. Bubbly ice is equivalent to B-type (bubbly) ice defined by Kameda et al. (1993) or bubbly ice described by Vallon et al. (1976). Clear ice is equivalent to T-type (transparent) ice defined by Kameda et al. (1993) and blue ice described by Vallon et al. (1976).

We used borehole dilution tests in open boreholes (filled with water below the water table) left from firn core collection to determine rates of horizontal fluid movement within the aquifer (Drost et al., 1968; Havely et al., 1967; Jamin et al., 2015). First, we measured the background (preinjection) specific conductance of the liquid water in the open boreholes at 30 cm intervals starting at the water table using a Hydrolab. Then we injected a dilute saltwater solution (10 g salt in 1 L water, resulting in a specific conductance around ~130 μS/cm in a borehole with a 20 m saturated thickness) into the borehole and mixed it into the water in the borehole using a submersible well pump (12 V Tornado pump by Proactive). Then we monitored the specific conductance at 30 cm depth intervals every few hours over ~24 h. Within a 50 m borehole, 30 cm vertical resolution captures the medium and large scale horizontal flow patterns. However, it does not capture variability associated with stratigraphic changes smaller than 30 cm. Background specific conductance values in the borehole were 1–18 μS/cm. After saltwater injection, specific conductance values increased to ~100–200 μS/cm.

The dilution tests provide profiles of flow within the aquifer that we compare to theoretical flow estimates based on Darcy's law, which describes the flow of a fluid through porous media. The specific discharge within an aquifer can be calculated as

$$q = \frac{-\pi r}{2t\alpha} \ln\left(\frac{C}{C_o}\right) \tag{1}$$

where q is the specific discharge (length/time), r is the borehole radius (length), t is time, α is a formation factor accounting for the attenuation of the velocity field by the borehole, commonly taken to be equal to 2 (Pitrak et al., 2007), and C/C_o is the relative concentration at a given time. The specific discharge is the flow of water per unit area of porous media (SI units of $m^3/(m^2\ s)$) and refers to the flux of water flowing through an area of the porous medium, even though the water only flows through connected pores. Average linear velocity describes the velocity at which a tracer in the water would move (equation (S1) in the SI). Thus, the actual velocity of the water flowing through connected pores will differ from the specific discharge.

The calculated flow does not account for vertical flow or diffusion. Vertical flow within the borehole and molecular diffusion are ~100 times less than measured horizontal flow based on vertical hydraulic gradient measurements that were below detection and the characteristic diffusion length over the period of observation. Vertical hydraulic gradients calculated by the steel tape method (accurate to 0.003 m) were too small to detect (Cunningham & Schalk, 2011). Based on 0°C (±0.2°C) temperature measurements throughout the borehole, we assume temperature driven flow is negligible and that diffusion will also be reduced. We do not expect dilution by surface meltwater to influence salinity on the timescales of this test as maximum melt rates were ~1 mm/h (maximum addition of only 0.2% of water in borehole if sustained over 24 h). The mean residence time of water within the aquifer is calculated as

$$T = \frac{b \times \phi}{R} \tag{2}$$

where b is aquifer thickness (length), ϕ is porosity, and R is recharge rate (length/time) (Cook & Böhlke, 2000; Focazio et al., 1998). This calculation assumes that steady state flow conditions exist and aquifer thickness and recharge rates remain constant. The value of b is calculated from borehole dilution tests, porosity is estimated between 0.1 and 0.3 (Koenig et al., 2014), and recharge rates are estimated from weather station data at the field site (Miller, 2017).

3. Results

3.1. Dilution of Saltwater Over Time in Boreholes (Dilution Tests)

The background specific conductance within the boreholes prior to saltwater injection is shown in Figure 2. After the salt water injection, the specific conductance in the borehole at FA16_6 decreases with time above ~32 m, indicating dilution by freshwater flow through the borehole. The specific conductance eventually reaches background preinjection levels in 24 h. However, below ~32 m, the specific conductance remains

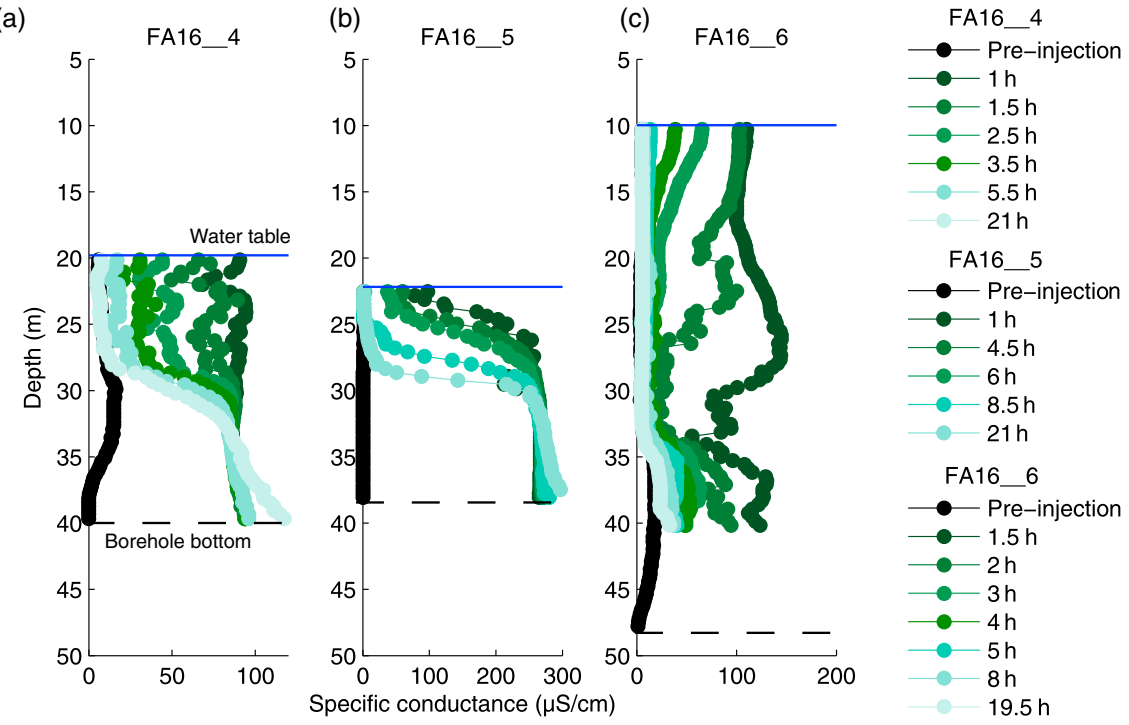

Figure 2. Plot showing dilution of injected salt water over time within boreholes due to freshwater flow. At FA16_4 the water table is at 20 m (a). Specific conductance returns to background levels in ~21 h within the flow zone (20–32 m). Below 32 m no dilution occurs, indicating that no water flow occurs. Dilution also occurs at (b) FA16_5 and (c) FA16_6.

at the initial postinjection level and does not return to the background value during our observation period (~24 h due to limited field time), indicating little to no freshwater flow. The specific conductance profile at FA16_5 also shows dilution at shallower depths and no dilution at greater depths, similar to FA16_4.

The specific conductance profile at FA16_6 shows a decrease in specific conductance at all depths we measured specific conductance at. We initially measured background specific conductance along the entire borehole, which was deep enough to observe specific conductance values of 1 μS/cm at the bottom of the borehole. Due to limited field time, we only measured specific conductance down to ~40 m during the dilution test because we incorrectly assumed that the clear ice defined the bottom of the aquifer and that measurements below 40 m, where the ice cores showed thick clear ice layers (Figure 3), were below the bottom of the aquifer.

The specific conductance increases unusually between 35 and 40 m at 21 h at FA16_4 and FA16_5. However, within 6 h, the increase is less that 10 μS/cm, and within 21 h, it is only 25 μS/cm, so the change is small and has little influence on the overall dilution rates because they are based on the dilution at each time interval. During the initial saltwater injection and mixing, some higher salinity water may have flowed to the bottom of the borehole, below the intake of the pump at the bottom of the borehole. When we removed the pump at the end of the day (after the measurements at 5.5 h at FA16_4 and 8.5 h at FA16_5), we could have mixed some higher salinity water up into the borehole that we see in our final depth-profile measurement after 21 h.

3.2. Specific Discharge and the Bottom of the Flow Zone

Specific discharge and background specific conductance profiles within the aquifer are shown for the three sites (FA16_4, FA16_5, and FA16_6) in Figure 3. The specific discharge profiles reveal flow zones within the saturated firn. The water table defines the top of the aquifer, and the specific discharge decrease to zero defines the bottom of the aquifer. The thickness of the aquifer is the difference between the bottom depth and water table depth. A confining layer exists below the aquifer, where firn and ice may be saturated but no flow occurs. Table 1 provides a summary of aquifer depth and thickness within the ice sheet.

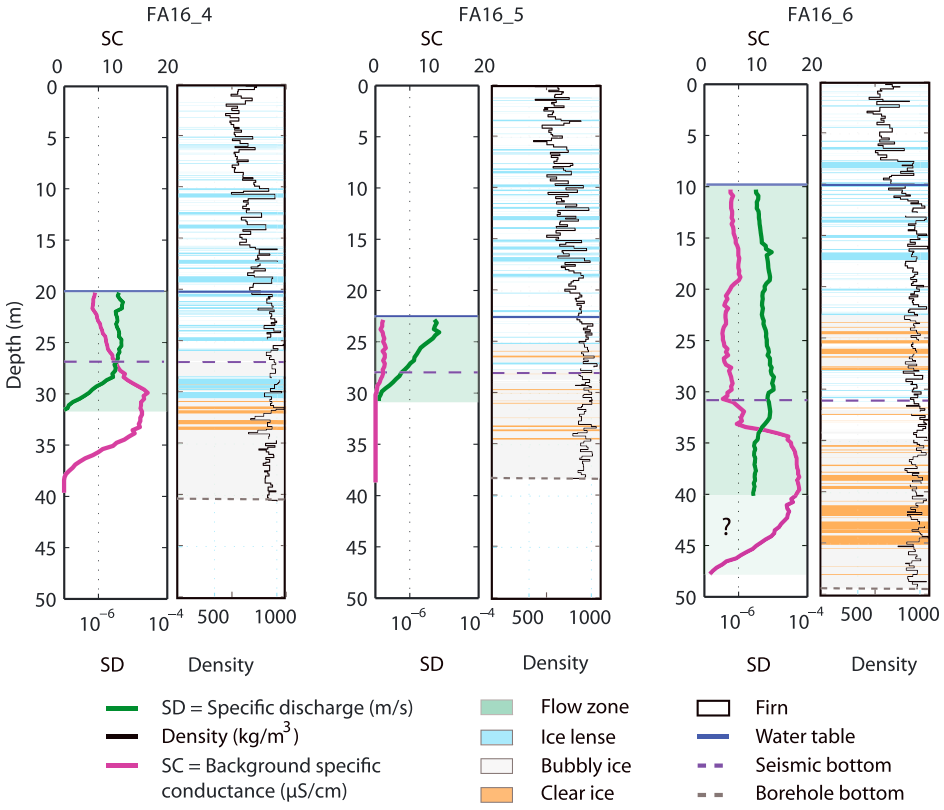

Figure 3. Plots showing the specific discharge (SD), background specific conductance prior to saltwater injection (SC), firn density, and stratigraphy, depth to the water table, and aquifer seismic bottom from seismic survey (from Montgomery et al., 2017) for sites where borehole dilution tests were performed. The flow zone is defined by positive specific discharge. The flow zone is not apparent in the density or stratigraphy profiles. The background specific conductance was measured twice at FA16_5 with similar results. At FA16_6 we measured the background specific conductance to the bottom of the borehole but only measured changes in specific discharge to ~40 m depth. The depth to the bottom of the flow zone is unknown at this site.

The specific discharge is highest at the top of the aquifer (~5×10^{-6} m/s) and generally decreases with depth toward the bottom (~1×10^{-7} m/s). Average and total specific discharge integrated over the aquifer thickness is shown in Table 1. Our specific conductance measurements during the borehole dilution test at site FA16_6 did not go deep enough to detect the bottom of the aquifer at FA16_6. Therefore, the average specific discharge at FA16_6 is likely an overestimates because the measurements stopped above the bottom of the flow zone and do not include the portion of the aquifer with lower specific discharge.

Table 1
Aquifer Geometry and Flow Rates

Site	FA16_4			FA16_5			FA16_6[a]		
Depth to water table (m)	20.14			22.53			9.98		
Depth to bottom of flow (m)	31.7			30.5			40.2–47.8		
Aquifer thickness (m)	11.6			8			30.2–37.8		
Average specific discharge (standard deviation) (m/s)	2.9×10^{-6} (1.5×10^{-6})			2.2×10^{-6} (2.2×10^{-6})			5.6×10^{-6} (2.2×10^{-6})		
Total discharge through flow zone (m^2/s)	3.3×10^{-5}			1.7×10^{-5}			1.7×10^{-4}		
For porosity	0.1	0.2	0.3	0.1	0.2	0.3	0.1	0.2	0.3
Average linear velocity (standard deviation) (m/d)	2.5 (1.4)	0.4 (0.2)	0.1 (0.0)	1.9 (1.9)	0.9 (1)	0.7 (0.6)	4.6 (1.3)	1.1 (0.4)	0.3 (0.1)

Note. Water table and aquifer bottom depths, average specific discharge, total specific discharge (per unit width of aquifer), and average linear velocity of water at each site. We did not measure changes in specific conductance deep enough to detect the bottom of flow at FA16_6. Therefore, we provide a range from the bottom of the background specific conductance measurements to the bottom of the specific discharge measurements. The total discharge is the specific discharge integrated over the thickness of the flow zone.
[a]The estimates at FA16_6 are likely an overestimate as we did not capture the bottom of the flow zone, where the specific discharge should be lower. Specific discharge calculated using Darcy's law is 2.7×10^{-6} m/s.

Although variations in specific discharge correspond to large scale stratigraphic changes (meters) within the firn core, the effect of ice stratigraphy and density on flow is low. The specific discharge where thick, clear ice layers occur and the firn density approaches that of glacier ice can be the same as the specific discharge through firn. This may be related to the lateral extent of ice layers. Even if they are impermeable locally, they may not be laterally extensive enough to prevent flow through layers below. Specific discharge measurements were made at 30 cm intervals, while some clear ice layers were thicker than 30 cm. The bottom of the flow zone flow cannot be determined from the core stratigraphy or density profiles alone.

The background specific conductance generally increases with depth to a peak (~coincident with the aquifer bottom) and then decreases near the bottom of the borehole. The maximum background specific conductance is 18 μS/cm at FA16_6. The bottom of the flow zone from the borehole dilution tests coincides with the depth that the background specific conductance goes to zero at FA16_5. At site FA16_4, these depths differ by 5 m (the background specific conductance goes to zero at ~37 m, while the specific discharge goes to zero at ~32 m). Flow and background specific conductance measurements at FA16_6 indicate that the bottom of the aquifer at this site is between 40 m to nearly 50 m depth.

3.3. Average Linear Velocity Profiles

We calculated average linear velocities to compare flow rates of liquid water to ice (see supporting information, equation (S1)). Assuming vertically uniform porosities between 0.1 and 0.3 (Koenig et al., 2014), the average linear velocity ranges from 0.1 to 4.6 m/d. The mean average linear velocities of meltwater for each site are shown in Table 1, calculated using site average specific discharge. The maximum average linear velocity, calculated using measured specific discharge at depth, is 9.2 m/d (FA16_6, assuming 10% porosity). In reality, porosity varies with depth due to compaction, but this estimate provides a range of realistic possible values. Porosity has been difficult to precisely measure at our site.

3.4. Mean Residence Time Estimates

The mean residence time describes the length of time it takes for water within the aquifer to recharge, travel through, and discharge from an aquifer. Water in the firn aquifer near Helheim Glacier has a relatively short residence time between 4 and 35 years for a porosity range of 0.1–0.3 and recharge rates between 10 and 30 cm/yr. Using an average porosity of 0.16 (Montgomery et al., 2017) and average recharge rate of 20 cm/yr, the residence time is 7–22 years. Higher porosities result in longer residence times. However, an average porosity of 0.3 throughout the aquifer is higher than observations indicate (Koenig et al., 2014; Montgomery et al., 2017), supporting shorter residence time estimates.

4. Discussion and Conclusions

During the borehole dilution tests in the firn aquifer, salt water mixed into the water-saturated part of an open borehole was diluted by water inflow through the borehole. Dilution of saltwater over time in the borehole indicates that the water within the aquifer flows and, therefore, discharges from the aquifer somewhere down hydraulic gradient. Continuity of mass requires that flow in an aquifer be accompanied by discharge and/or a change in storage. Working near the edge of the crevasses, there is not enough unsaturated firn to accommodate the volume of water flowing through the aquifer in the firn pore space and we have not observed surface discharge at our field site. Therefore, we conclude that meltwater discharges from the aquifer. Discharge from the aquifer most likely occurs in places where the firn aquifer intersects a downslope crevasse field as supported by radar imaging (Miège et al., 2016).

Darcy's law predicts a specific discharge of 2.7×10^{-6} m/s using a hydraulic conductivity estimated as 2.7×10^{-4} m/s (Miller et al., 2017) and a hydraulic gradient, determined from ground penetrating radar (Forster et al., 2014), of 0.01 m/m (slope = 0.8°). The specific discharge measurements from the borehole dilution tests (mean specific discharge of 4.3×10^{-6} m/s, standard deviation 2.5×10^{-6} m/s) generally agree with the specific discharge predicted by Darcy's law.

The water flowing through the ice is moving faster than the ice is flowing. The average linear velocity of water moving through the aquifer (0.1–4.6 m/d) is up to 10 times faster than the ice it flows through. The ice sheet surface velocity measured by GPS is between ~0.3 and .45 m/d (for 2015–2016).

The bottom depths identified in the specific discharge profiles agree with bottom depths determined from active source seismic surveys to estimate velocities associated with the base of the aquifer for two out of three sites (seismic bottom in Figure 3) (Montgomery et al., 2017). The site where the two methods disagree is the lowest elevation site (1519 m), where the aquifer has likely existed for a longer time (assuming it formed at lower elevations where temperatures are warmer and based on observed inland expansion) (Montgomery et al., 2017). The seismic method is sensitive to the presence of clear ice, which is greater at this site than the other two sites, likely contributing to differences in the bottom depth estimates. The bottom of the aquifer is not apparent from ice core stratigraphy or density observations alone.

Firn can serve as a substantial storage reservoir for meltwater (Harper et al., 2012; Humphrey et al., 2012). However, flow within the firn aquifer suggests that in areas where firn aquifers occur, storage is short term (residence time $<$30 years). Meltwater discharge, possibly to the ocean, may actually be enhanced relative to unsaturated firn because instead of refreezing within firn pore space, meltwater drains out of the aquifer. Firn storage at this location has already reached 50% of capacity based on firn density profiles (Koenig et al., 2014). The saturation of the pore space maximizes hydraulic conductivity (Freeze & Cherry, 1979) and allows meltwater generated inland to travel faster, and further, toward the edge of the ice sheet than if the meltwater were flowing through unsaturated firn. The insulating properties of the thick overlying firn prevent the meltwater from refreezing, resulting in a perennial mechanism for meltwater originating tens of kilometers from the edge of the ice sheet to connect with the englacial hydrologic system closer to the edge, and runoff. Although the firn contains a large storage capacity, the firn aquifer and its connection to the broader glacial hydrologic system allows meltwater to flow out of the firn, thus reducing storage duration.

In southeast Greenland, meltwater recharges the aquifer, travels through the saturated zone, and flows out of the aquifer, likely into crevasses at the edge of the ice sheet, where it may refreeze or eventually reach the ocean. The observed flow favors the first hypothesis described in section 1 that aquifers drain into the broader hydrologic system. Meltwater flowing into crevasses may flow to the base of the ice sheet and influence ice dynamics by enhancing basal melt (Parizek & Alley, 2004) and basal sliding, leading to increased ice velocity and discharge to the ocean (Alley et al., 2005; Koenig et al., 2014; Poinar et al., 2017; Zwally, 2002). While the aquifer water has the potential to reach the subglacial hydrologic network via crevasses (Poinar et al., 2017), the specific pathways, processes, and timing of meltwater after it discharges from the aquifer have not been determined. Further study is required to fully quantify rates and timing of flow into crevasses, possible transport to the ice sheet base, and the effects on ice sheet dynamics, mass balance, and sea level rise.

Acknowledgments
This work was supported by NSF grant PLR-1417987. N. S. was supported by PLR-1417993. L. K. was supported by NASA Cryospheric Sciences program NASA award NNX15AC62G. S. L. was supported by an NOW ALW Veni grant 865.15.023. The authors thank Kyli Cosper, Kathy Young, and the entire CH2M Polar Field Services team for logistical assistance. Thanks also to Jay Kyne for drill consultation and development. The authors declare that the research was conducted in the absence of any commercial or financial relationships that could be construed as a potential conflict of interest. The data used are listed in the references, figures, and tables, and supporting information.

References

Alley, R. B., Dupont, T. K., Parizek, B. R., & Anandakrishnan, S. (2005). Access of surface meltwater to beds of sub-freezing glaciers: Preliminary insights. *Annals of Glaciology*, *40*, 8–14. https://doi.org/10.3189/172756405781813483

Burgess, E. W., Forster, R. R., Box, J. E., Mosley-Thompson, E., Bromwich, D. H., Bales, R. C., & Smith, L. C. (2010). A spatially calibrated model of annual accumulation rate on the Greenland Ice Sheet (1958–2007). *Journal of Geophysical Research*, *115*, F02004. https://doi.org/10.1029/2009JF001293

Chu, V. W. (2014). Greenland ice sheet hydrology: A review. *Progress in Physical Geography*, *38*(1), 19–54. https://doi.org/10.1177/0309133313507075

Cogley, J. G., Hock, R., Rasmussen, L. A., Arendt, A. A., Bauder, A., Braithwaite, R. J., … Zemp, M. (2011). *Glossary of glacier mass*, International Hydrological Programme,United Nations Eductional Scientific and Cultural Organization, Paris 86, 114.

Cook, P. G., & Böhlke, J.-K. (2000). Determining timescales for groundwater flow and solute transport. In *Environmental tracers in subsurface hydrology* (pp. 1–30). Boston, MA: Springer. https://doi.org/10.1007/978-1-4615-4557-6_1

Cunningham, W. L., & Schalk, C. W. (2011). Groundwater technical procedures of the U.S. Geological Survey: U.S. Geological Survey Techniques and Methods 1–A1, 151.

de la Peña, S., Howat, I. M., Nienow, P. W., van den Broeke, M. R., Mosley-Thompson, E., Price, S. F., … Sole, A. J. (2015). Changes in the firn structure of the western Greenland Ice Sheet caused by recent warming. *The Cryosphere*, *9*(3), 1203–1211. https://doi.org/10.5194/tc-9-1203-2015

Drost, W., Klotz, D., Koch, A., Moser, H., Neumaier, F., & Rauert, W. (1968). Point dilution methods of investigating ground water flow by means of radioisotopes. *Water Resources Research*, *4*(1), 125–146. https://doi.org/10.1029/WR004i001p00125

Enderlin, E. M., Howat, I. M., Jeong, S., Noh, M.-J., van Angelen, J. H., & van den Broeke, M. R. (2014). An improved mass budget for the Greenland ice sheet. *Geophysical Research Letters*, *41*, 866–872. https://doi.org/10.1002/2013GL059010

Ettema, J., van den Broeke, M. R., van Meijgaard, E., van de Berg, W. J., Bamber, J. L., Box, J. E., & Bales, R. C. (2009). Higher surface mass balance of the Greenland ice sheet revealed by high-resolution climate modeling. *Geophysical Research Letters*, *36*, L12501. https://doi.org/10.1029/2009GL038110

Fettweis, X., Tedesco, M., Van Den Broeke, M., & Ettema, J. (2011). Melting trends over the Greenland ice sheet (1958–2009) from spaceborne microwave data and regional climate models. *The Cryosphere*, *5*(2), 359–375. https://doi.org/10.5194/tc-5-359-2011

Focazio, M. J., Plummer, L. N., Bohlke, J. K., Busenberg, E., Bachman, L. J., & Powars, D. S. (1998). Preliminary estimates of residence times and apparent ages of ground water in the Chesapeake Bay watershed, and water- quality data from a survey of springs. In *Investigations Report 97-4225*.

Forster, R. R., Box, J. E., Van Den Broeke, M. R., Miège, C., Burgess, E. W., Van Angelen, J. H., … McConnell, J. R. (2014). Extensive liquid meltwater storage in firn within the Greenland ice sheet. *Nature Geoscience*, *7*(2), 1–4. https://doi.org/10.1038/ngeo2043

Freeze, A., & Cherry, J. (1979). *Groundwater*. Englewood Cliffs, NJ: Prentice Hall.

Hall, D. K., Comiso, J. C., DiGirolamo, N. E., Shuman, C. A., Box, J. E., & Koenig, L. S. (2013). Variability in the surface temperature and melt extent of the Greenland ice sheet from MODIS. *Geophysical Research Letters*, *40*, 2114–2120. https://doi.org/10.1002/grl.50240

Harper, J., Humphrey, N., Pfeffer, W. T., Brown, J., & Fettweis, X. (2012). Greenland ice-sheet contribution to sea-level rise buffered by meltwater storage in firn. *Nature*, *491*(7423), 240–243. https://doi.org/10.1038/nature11566

Havely, E., Moser, H., Zellhofer, O., & Zuber, A. (1967). Borehole dilution techniques: A critical review isotopes. In *Isotopes in hydrology, International atomic energy agency* (pp. 531–564). Vienna, Austria.

Helm, V., Humbert, A., & Miller, H. (2014). Elevation and elevation change of Greenland and Antarctica derived from CryoSat-2. *The Cryosphere*, *8*(4), 1539–1559. https://doi.org/10.5194/tc-8-1539-2014

Humphrey, N. F., Harper, J. T., & Pfeffer, W. T. (2012). Thermal tracking of meltwater retention in Greenland's accumulation area. *Journal of Geophysical Research*, *117*, F01010. https://doi.org/10.1029/2011JF002083

Jamin, P., Goderniaux, P., Bour, O., Le Borgne, T., Englert, A., Longuevergne, L., & Brouyère, S. (2015). Contribution of the finite volume point dilution method for measurement of groundwater fluxes in a fractured aquifer. *Journal of Contaminant Hydrology*, *182*, 244–255. https://doi.org/10.1016/j.jconhyd.2015.09.002

Kameda, T., Takahashi, S., Goto-Azuma, K., Kohshima, S., Watanabe, O., & Hagen, J. O. (1993). First report of ice core analyses and borehole temperatures on the highest icefield on western Spitsbergen in 1992. *Bulletin of Glacier Research*, *11*, 51–61.

Koenig, L. S., Lampkin, D. J., Montgomery, L. N., Hamilton, S. L., Turrin, J. B., Joseph, C. A., … Gogineni, P. (2015). Wintertime storage of water in buried supraglacial lakes across the Greenland Ice Sheet. *The Cryosphere*, *9*(4), 1333–1342. https://doi.org/10.5194/tc-9-1333-2015

Koenig, L. S., Miege, C., Forster, R. R., & Brucker, L. (2014). Initial in situ measurements of perennial meltwater storage in the Greenland firn aquifer. *Geophysical Research Letters*, *41*, 81–85. https://doi.org/10.1002/2013GL058083

Kuipers Munneke, P., Ligtenberg, S. R. M., van den Broeke, M. R., van Angelen, J. H., & Forster, R. R. (2014). Explaining the presence of perennial liquid water bodies in the firn of the Greenland Ice Sheet. *Geophysical Research Letters*, *41*, 476–483. https://doi.org/10.1002/2013GL058389

Lewis, S. M., & Smith, L. C. (2009). Hydrologic drainage of the Greenland ice sheet. *Hydrological Processes*, *23*(14), 2004–2011. https://doi.org/10.1002/hyp.7343

Lindbäck, K., Pettersson, R., Hubbard, A. L., Doyle, S. H., van As, D., Mikkelsen, A. B., & Fitzpatrick, A. A. (2015). Subglacial water drainage, storage, and piracy beneath the Greenland ice sheet. *Geophysical Research Letters*, *42*, 7606–7614. https://doi.org/10.1002/2015GL065393

Machguth, H., MacFerrin, M., van As, D., Box, J. E., Charalampidis, C., Colgan, W., … van de Wal, R. S. W. (2016). Greenland meltwater storage in firn limited by near-surface ice formation. *Nature Climate Change*, *6*(4), 390–393. https://doi.org/10.1038/nclimate2899

Miège, C., Forster, R. R., Box, J. E., Burgess, E. W., Mcconnell, J. R., Pasteris, D. R., & Spikes, V. B. (2013). Southeast Greenland high accumulation rates derived from firn cores and ground-penetrating radar. *Annals of Glaciology*, *54*(63), 322–332. https://doi.org/10.3189/2013AoG63A358

Miège, C., Forster, R. R., Brucker, L., Koenig, L. S., Solomon, D. K., Paden, J. D., … Gogineni, S. (2016). Spatial extent and temporal variability of Greenland firn aquifers detected by ground and airborne radars. *Journal of Geophysical Research: Earth Surface*, *121*, 2381–2398. https://doi.org/10.1002/2016JF003869

Miller, O. L. (2017). Hydrology of a firn aquifer in southeast Greenland, University of Utah.

Miller, O. L., Solomon, D. K., Miège, C., Koenig, L. S., Forster, R. R., Montgomery, L. N., … Brucker, L. (2017). Hydraulic conductivity of a firn aquifer in southeast Greenland. *Frontiers in Earth Science*, *5*, 38. https://doi.org/10.3389/feart.2017.00038

Montgomery, L. N., Schmerr, N., Burdick, S., Forster, R. R., Koenig, L., Ligtenberg, S., … Legchenko, A. (2017). Investigation of firn aquifer structure in southeastern Greenland using active source seismology. *Frontiers in Earth Science*, *5*, 10. https://doi.org/10.3389/FEART.2017.00010

Parizek, B. R., & Alley, R. B. (2004). Implications of increased Greenland surface melt under global-warming scenarios: Ice-sheet simulations. *Quaternary Science Reviews*, *23*(9-10), 1013–1027. https://doi.org/10.1016/j.quascirev.2003.12.024

Parry, V., Nienow, P., Mair, D., Scott, J., Hubbard, B., Steffen, K., & Wingham, D. (2007). Investigations of meltwater refreezing and density variations in the snowpack and firn within the percolation zone of the Greenland ice sheet. *Annals of Glaciology*, *46*, 61–68. https://doi.org/10.3189/172756407782871332

Pfeffer, W. (1991). Retention of Greenland runoff by refreezing: Implications for projected future sea level change. *Journal of Geophysical Research*, *96*(C12), 22,117. https://doi.org/10.1029/91JC02502

Pitrak, M., Mares, S., & Kobr, M. (2007). A simple borehole dilution technique in measuring horizontal ground water flow. *Ground Water*, *45*(1), 89–92. https://doi.org/10.1111/j.1745-6584.2006.00258.x

Poinar, K., Joughin, I., Lilien, D., Brucker, L., Kehrl, L., & Nowicki, S. (2017). Drainage of Southeast Greenland firn aquifer water through crevasses to the bed. *Frontiers in Earth Science*, *5*, 5. https://doi.org/10.3389/FEART.2017.00005

Rennermalm, A. K., Smith, L. C., Chu, V. W., Box, J. E., Forster, R. R., Van Den Broeke, M. R., … Moustafa, S. E. (2013). Evidence of meltwater retention within the Greenland ice sheet. *The Cryosphere*, *7*(5), 1433–1445. https://doi.org/10.5194/tc-7-1433-2013

Shepherd, A., Ivins, E. R., A, G., Barletta, V. R., Bentley, M. J., Bettadpur, S., … Zwally, H. J. (2012). A reconciled estimate of ice-sheet mass balance. *Science*, *338*(6111), 1183–1189. https://doi.org/10.1126/science.1228102

Smith, L. C., Chu, V. W., Yang, K., Gleason, C. J., Pitcher, L. H., Rennermalm, A. K., … Balog, J. (2015). Efficient meltwater drainage through supraglacial streams and rivers on the southwest Greenland ice sheet. *Proceedings of the National Academy of Sciences of the United States of America*, *112*(4), 1001–1006. https://doi.org/10.1073/pnas.1413024112

Steger, C. R., Reijmer, C. H., van den Broeke, M. R., Wever, N., Forster, R. R., Koenig, L. S., … Noël, B. P. Y. (2017). Firn meltwater retention on the Greenland ice sheet: A model comparison. *Frontiers in Earth Science*, *5*, 3. https://doi.org/10.3389/FEART.2017.00003

Tedesco, M. (2013). Evidence and analysis of 2012 Greenland records from spaceborne observations, a regional climate model and reanalysis data. *The Cryosphere*, *7*(2), 615–630. https://doi.org/10.5194/tc-7-615-2013

Vallon, M., Petit, J.-R., & Fabre, B. (1976). Study of an ice core to the bedrock in the accumulation zone of an Alpine glacier. *Journal of Glaciology*, *17*(75), 13–28. https://doi.org/10.1017/S0022143000030677

van Angelen, J. H., Lenaerts, J. T. M., Lhermitte, S., Fettweis, X., Kuipers Munneke, P., van den Broeke, M. R., … Smeets, C. J. P. P. (2012). Sensitivity of Greenland ice sheet surface mass balance to surface albedo parameterization: A study with a regional climate model. *The Cryosphere*, *6*(5), 1175–1186. https://doi.org/10.5194/tc-6-1175-2012

van Angelen, J. H., Lenaerts, J. T. M., van den Broeke, M. R., Fettweis, X., & van Meijgaard, E. (2013). Rapid loss of firn pore space accelerates 21st century Greenland mass loss. *Geophysical Research Letters*, *40*, 2109–2113. https://doi.org/10.1002/grl.50490

van den Broeke, M., Bamber, J., Ettema, J., Rignot, E., Schrama, E., van de Berg, W. J., … Wouters, B. (2009). Partitioning recent Greenland mass loss. *Science*, *326*(5955), 984–986. https://doi.org/10.1126/science.1178176

Vaughan, D. G., Comiso, J. C., Allison, I., Carrasco, J., Kaser, G., Kwok, R., & Mote, P. (2013). Observations: Cryosphere. In V. B. Stocker, et al. (Eds.), *Climate change 2013—The physical science basis: Contribution working group I to Fifth Assessment Report Intergovernmental Panel on Climate Change* (pp. 317–382). Cambridge, United Kingdom and New York: Cambridge University Press. https://doi.org/10.1017/CBO9781107415324.012

Zwally, H. J. (2002). Surface melt-induced acceleration of Greenland ice-sheet flow. *Science*, *297*(5579), 218–222. https://doi.org/10.1126/science.1072708